Correlations, quantum entanglement and interference in nanoscopic systems

J. Stat. Mech. (2010) P11031

(http://iopscience.iop.org/1742-5468/2010/11/P11031)

Journal of Statistical Mechanics: Theory and Experiment
An IOP and SISSA journal

Correlations, quantum entanglement and interference in nanoscopic systems

K Hallberg[1], Julián Rincón[1], M Nizama[1], A A Aligia[1] and S Ramasesha[2]

[1] Centro Atómico Bariloche and Instituto Balseiro, Comisión Nacional de Energía Atómica and CONICET, 8400 Bariloche, Argentina
[2] Solid State and Structural Chemistry Unit, Indian Institute of Science, Bangalore 560 012, India
E-mail: karenhallberg@gmail.com, julian.jimenez@cab.cnea.gov.ar, marco.nizama@cab.cnea.gov.ar, aligia@cab.cnea.gov.ar and ramasesh@sscu.iisc.ernet.in

Received 27 October 2010
Accepted 28 October 2010
Published 19 November 2010

Online at stacks.iop.org/JSTAT/2010/P11031
doi:10.1088/1742-5468/2010/11/P11031

Abstract. Several of the most interesting quantum effects can or could be observed in nanoscopic systems. For example, the effect of strong correlations between electrons and of quantum interference can be measured in transport experiments through quantum dots, wires, individual molecules and rings formed by large molecules or arrays of quantum dots. In addition, quantum coherence and entanglement can be clearly observed in quantum corrals.

In this paper we present calculations of transport properties through Aharonov–Bohm strongly correlated rings where the characteristic phenomenon of charge–spin separation is clearly observed. Additionally quantum interference effects show up in transport through π-conjugated annulene molecules producing important effects on the conductance for different source–drain configurations, leading to the possibility of an interesting switching effect.

Finally, elliptic quantum corrals offer an ideal system to study quantum entanglement due to their focalizing properties. Because of an enhanced interaction between impurities localized at the foci, these systems also show interesting quantum dynamical behaviour and offer a challenging scenario for quantum information experiments.

Keywords: mesoscopic systems (theory), entanglement in extended quantum systems (theory), quantum transport in one dimension

1742-5468/10/P11031+15$30.00

Contents

1. Introduction 2
2. Transport through nanoscopic systems 3
2.1. How spin and charge could be observed independently in interacting systems 3
2.2. Quantum interference in transport through molecules 5
3. Entanglement in confined quantum systems 7
4. Conclusions 13
Acknowledgments 13
References 14

1. Introduction

New advances in nanotechnology led to the fabrication of different nanostructures, motivated either by technological interest or the possibility of testing theories for strongly correlated electrons and observing new phenomena. One example is the realization of the Kondo effect in systems with one quantum dot (QD) [1]–[4] and the study of universal properties in non-equilibrium transport [5]–[8]. Another one is a study of the metal–insulator transition in a chain of several QDs [9]. Systems of a few QDs have been proposed theoretically as realizations of the two-channel Kondo model [10, 11], the so-called ionic Hubbard model [12] and the double exchange mechanism [13]. Recently it has been studied how the Kondo resonance splits in two in a system of two QDs, one of them non-interacting [14, 15].

Several interesting properties arise from artificial and molecular systems. On the one hand, artificial nanorings of nanoladders with strong interacting electrons could be assembled to observe the elusive property of charge–spin separation (SCS), characteristic of strongly correlated low-dimensional systems [16].

In addition, molecular systems also pose a challenging scenario for transport experiments as seen from various successful attempts [17]–[19]. The possibility of achieving controlled quantum transport has been studied, for example in electronic conductance through single π-conjugated molecules using theoretical [20]–[25] and experimental [26]–[29] techniques.

Other relevant nanoscopic systems with interesting quantum properties are the so-called quantum corrals. Here the electrons remain quantically confined by means of a geometrical array of adatoms deposited on the surface of noble metals, forming a nearly closed structure. These systems have allowed the observation of surprising effects such as quantum mirages [30]–[32]: a 'ghost' image in one focus of an elliptical quantum corral was measured by deposition of an impurity on the other focus. These systems are excellent candidates for technological applications in quantum information and spintronics [33, 34]. For example, by adding a magnetic atom on one focus the quantum mirage could be used as a geometric protection of magnetic qubits against decoherence. In addition, quantum

J. Stat. Mech. (2010) P11031

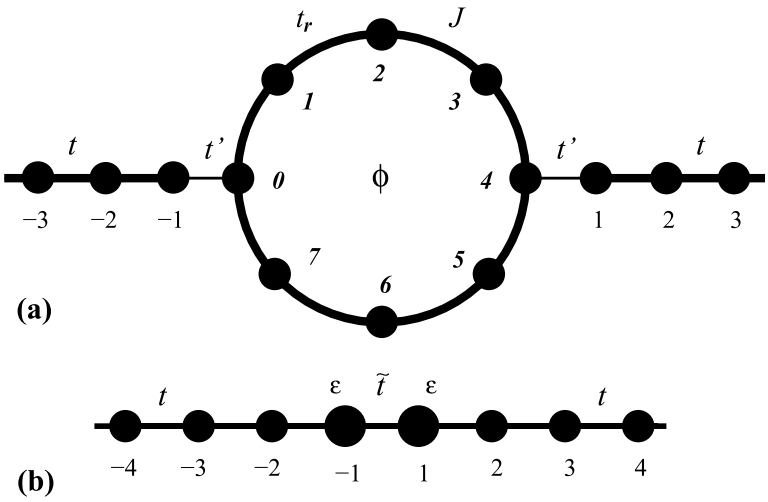

Figure 1. Sketch of the Aharonov–Bohm interacting ring modelled in the calculations (a) and its effective 1D version for small coupling to the leads.

entanglement can be robust if two magnetic impurities are added at the foci. Also feasible is the implementation of logic gates of one and two qubits. In this case, these corrals could serve as elementary prototypes of quantum computers.

2. Transport through nanoscopic systems

2.1. How spin and charge could be observed independently in interacting systems

Among the theoretical methods for detecting and visualizing SCS, predicted theoretically for one-dimensional strongly interacting systems, direct calculations of the real-time evolution of electronic wavepackets in finite Hubbard rings revealed different velocities in the dispersion of spin and charge densities as an immediate consequence of SCS [16]. Also, Kollath *et al* [35] have repeated this calculation for larger systems using the density matrix renormalization group (DMRG) technique [36] and observed distinct features of SCS in a model for one-dimensional cold Fermi gases in a harmonic trap, proposing quantitative estimates for an experimental observation of SCS in an array of atomic wires.

In [37] and [38], the transmission through infinite Aharonov–Bohm (AB) rings was analysed. The dynamics of the electrons in the ring was described by a Luttinger liquid (LL) propagator with different charge and spin velocities, v_c and v_s, included explicitly. They found that the flux dependence of the transmission has, in addition to the periodicity in multiples of the flux quantum $\Phi_0 = hc/e$, new structures which appear at fractional values of the flux. In addition, numerical calculations of the transmittance through finite AB rings described by the t–J and Hubbard models show clear dips at the fluxes that correspond to the ratio v_s/v_c [39]–[42]. The extension of these results to ladders of two legs was also considered, as a first step to higher dimensions [43].

The system considered is sketched in figure 1. It consists of an interacting ring weakly coupled to two non-interacting leads. Our model Hamiltonian is $H = H_{\rm leads} + H_{\rm link} + H_{\rm ring}$,

where $H_{\rm leads}$ describes free electrons in the left and right leads,

$$H_{\rm link} = -t' \sum_{\sigma} (a^{\dagger}_{-1,\sigma} c_{L,\sigma} + a^{\dagger}_{1,\sigma} c_{R,\sigma} + \text{H.c.}) \tag{1}$$

describes the exchange of quasiparticles between the leads ($a_{i,\sigma}$) and particular sites of the ring and $H_{\rm ring}$ depends on the modelling of the ring of L sites:

$$H_{\rm ring} = -eV_{\rm g} \sum_{l,\sigma} c^{\dagger}_{l,\sigma} c_{l,\sigma} - t \sum_{l,\sigma} (c^{\dagger}_{l,\sigma} c_{l+1,\sigma} \mathrm{e}^{-\mathrm{i}\phi/L} + \text{H.c.}) + H_{\rm int} \tag{2}$$

where the flux is given in units of the flux quantum $\phi = 2\pi\Phi/\Phi_0$ and the system is subjected to an applied gate voltage $V_{\rm g}$.

Several interacting electronic models can be considered for the ring. We have considered the paradigmatic Hubbard and t–J models. For the Hubbard model $H_{\rm int} = \sum_{l,\sigma\neq\sigma'} U n_{l,\sigma} n_{l,\sigma'}$, with $n_{l,\sigma} = c^{\dagger}_{l,\sigma} c_{l,\sigma}$. This model is also related to the well-known t–J model for very large interactions by $J = 4t^2/U$. We measure energies in units of t.

Following [37], the transmission from the left to the right lead can be calculated to second order in t', where the resulting effective Hamiltonian is equivalent to a one-particle model for a non-interacting chain with two central sites modified by the interacting ring, with effective on-site energy $\epsilon(\omega) = t'^2 G^{\rm R}_{\rm L,L}(\omega)$ and effective hopping between them $\tilde{t}(\omega) = t'^2 G^{\rm R}_{\rm L,R}(\omega)$. $G^{\rm R}_{i,j}(\omega)$ denotes the Green's function of the isolated ring.

By using the effective impurity problem, the transmittance and conductance of the system at zero temperature may then be computed. The transmittance $T(\omega)$ is given by [37]

$$T(\omega, V_{\rm g}, \phi) = \frac{4t^2 \sin^2 k |\tilde{t}(\omega)|^2}{|[\omega - \epsilon(\omega) + t\mathrm{e}^{\mathrm{i}k}]^2 - |\tilde{t}^2(\omega)||^2}, \tag{3}$$

where $\omega = -2t\cos k$ is the tight-binding dispersion relation for the free electrons in the leads which are incident upon the impurities. These equations are exact for a non-interacting system.

From equation (3), $T(\omega, V_{\rm g}, \phi)$ can be calculated from the Green's functions of the isolated ring. We consider holes incident on a ring of L sites and $N = N_e + 1$ electrons in the ground state, obtaining the Green's functions from the ground state of the ring calculated using numerical diagonalization [44]. Then we substitute these in equation (3). We fix the energy $\omega = 0$ to represent half-filled leads and explore the dependence of the transmittance on the threading flux, obtained by integration over the excitations in a small energy window, which accounts for possible voltage fluctuations and temperature effects [39].

For infinite on-site repulsion U (or equivalently $J = 0$), the wavefunction can be factorized into a spin and a charge part [39, 45, 46]. Therefore, charge–spin separation becomes evident for finite systems and independent of system size. For each spin state, the system can be mapped into a spinless model with an effective flux which depends on the spin. Considering a non-degenerate ground state containing $N = N_e + 1$ particles and analysing the part of the Green's function that enters the transmittance when a particle is destroyed, it is shown that the dips occur when two intermediate states cross at a given flux and interfere destructively. These particular fluxes depend on the spin quantum numbers and are located at [40]

$$\phi_d = \pi(2n+1)/N_e, \tag{4}$$

J. Stat. Mech. (2010) P11031

with n integer. If the integration energy window includes these levels, a dip in the conductance arises.

In figure 2 we show results for the transmittance using the t–J (top) and Hubbard (bottom) models in the ring. For large interactions, $J \ll t$ or $U \gg t$, dips are found at the positions given by equation (4). However, when J is enlarged or U is reduced, increasing the mixture between different spin sectors, the spin–charge separation is affected and we observe the appearance of new dips and a shift of some of them. This is because the destructively interfering level crossings which lead to the reduction in the conductance occur at different values of the flux, as explained in [40].

2.2. Quantum interference in transport through molecules

Quantum interference might play a crucial role in transport measurement through molecules and could be used as a handle to control conductance through such systems. In recent theoretical works [20, 23, 24], the idea of a quantum interference effect transistor (QuIET) based on single annulene molecules, including benzene, was proposed. The equilibrium conductance at zero bias and gate voltage (V_g) was calculated in the last two papers for the strong coupling limit using the non-equilibrium Green's function and the Landauer–Büttiker formalism. However, as annulenes have a gap at an energy corresponding to $V_g = 0$ due mainly to the strong Coulomb interactions present in the molecule, for zero gate voltage the conductance is finite, albeit small, only for strong coupling to the leads. For weak coupling the conductance will be appreciable only through the main channels of the molecule which are a few electronvolts away from the Fermi energy. By analysing the QuIET at the main transmittance channels the switching effect is be much more pronounced and robust [20].

We have studied annular π-conjugated molecules with N sites, weakly connected to non-interacting leads in the A or B configurations (figure 3). Now the interacting Hamiltonian $H_{\rm ring}$ describes the isolated π-conjugated molecule, modelled by the PPP Hamiltonian [47], with on-site energy given by a gate voltage V_g:

$$H_{\rm ring} = -eV_g \sum_{i=1,\sigma}^{N} c_{i\sigma}^{\dagger} c_{i\sigma} - t \sum_{\langle ij\rangle,\sigma} c_{i\sigma}^{\dagger} c_{j\sigma} + \sum_i U_i (n_{i\downarrow} - \tfrac{1}{2})(n_{i\uparrow} - \tfrac{1}{2}) + \sum_{i>j} V_{ij}(n_i - 1)(n_j - 1) \tag{5}$$

where the operators $c_{i\sigma}^{\dagger}$ ($c_{i\sigma}$) create (annihilate) an electron of spin σ in the π orbital of the carbon atom at site i, n are the corresponding number operators and $\langle \cdots \rangle$ stands for bonded pairs of carbon atoms. The intersite interaction potential V_{ij} is parametrized to interpolate between U and e^2/r_{ij} in the limit $r_{ij} \longrightarrow \infty$ [48]. In the Ohno interpolation, V_{ij} is given by $V_{ij} = U_i(1 + 0.6117 r_{ij}^2)^{-1/2}$, where the distance r_{ij} is in ångströms. The standard Hubbard parameter for sp^2 carbon is $U_i = 11.26$ eV and the hopping parameter t for $r = 1.397$ Å is 2.4 eV [49].

If we consider the isolated benzene molecule, which has translational symmetry, the allowed total momentum quantum numbers are $k = r\pi/3$, with r an integer. For a two-terminal set-up like the one considered here, wavefunctions travelling through both branches of the molecule will interfere producing different interference patterns depending

J. Stat. Mech. (2010) P11031

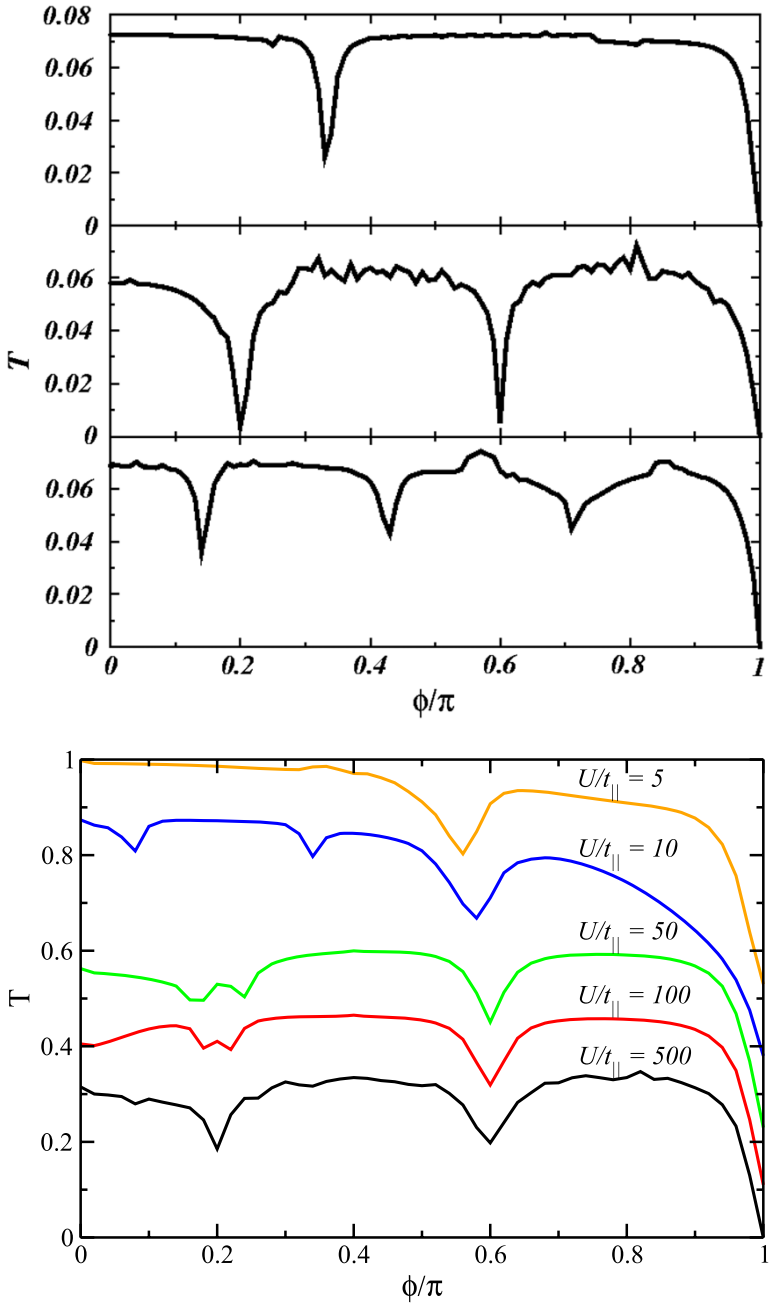

Figure 2. Transmittance versus flux. Top: t–J model for $J = 0.001$, $L = 8$ sites and $N_e + 1 = 4$, 6 and 8 from top to bottom. Bottom: Hubbard model with $L = 6$, $N_e + 1 = 6$ particles in the ground state and several values of U (curves are shifted vertically for better visualization).

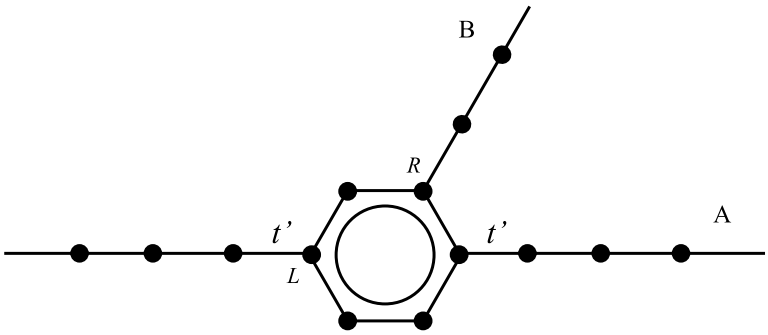

Figure 3. Schematic representation of the conjugate molecules considered for QuIETs with both relevant lead configurations mentioned in the text.

on the positions of the leads. The phase difference will be: $\Delta\phi = k\Delta x$ (in units of the C–C separation). For leads in the 'para' position, $\Delta x = 0$ and the waves are in phase, interfering constructively (figure 3, A configuration). However, in the 'meta' (B configuration) position ($\Delta x = 2$), the interference will depend on the k value of the particular channel. For the highest occupied molecular orbital (HOMO) and lowest unoccupied molecular orbital (LUMO) the phase differences will be $\Delta\phi = 2\pi/3$ and $\Delta\phi = 4\pi/3$, respectively, and the interference will reduce the amplitude in these channels.

In figure 4 we show results for the conductance through benzene molecules in the 'para' and 'meta' configurations of the leads. The nearly destructive interference effect for the latter case is clearly visible.

Considering that the reduction of the HOMO (or LUMO) peaks for the 'meta' configuration are due to destructive interference effects, one can ask whether disrupting translational invariance would lead to a larger conductance. This question was first addressed in [23] by introducing a local energy (Σ) at one site in benzene, focusing on the Fermi energy of the leads (set to zero) where the observed effect is small. In [20] we studied the effect of external perturbations on the main transmittance channels such as the HOMO and LUMO (away from the Fermi level) and we found a much larger response. These results are shown in the bottom part of figure 4, where an additional diagonal energy is added to the site to the right of the B ('meta') position (the effect is not qualitatively dependent on this position). It is clearly seen that, in this case, the small peak corresponding to the HOMO level develops and grows as the local energy is increased, disrupting the translational symmetry responsible for the destructive interference (see the inset). We also find that this effect is much more striking for larger annulenes. These results are not affected by molecular vibrations at room temperature since modes that can cause decoherence are excited at temperatures higher than 500 K [23].

3. Entanglement in confined quantum systems

There have been several papers analysing the beautiful experiments in quantum corrals [30]. One and two impurities have been considered in different configurations (see review articles in [31, 32]). In [32], [50]–[55] it was suggested that, as a consequence of the focalizing properties of quantum elliptic corrals, two impurities located at the foci

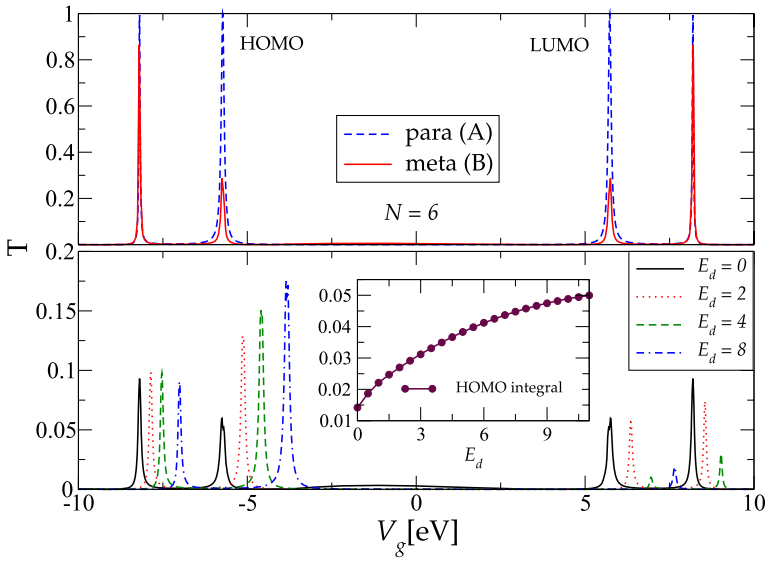

Figure 4. Top: conductance versus gate voltage (measured from the Fermi energy) through a benzene molecule for the 'para' or 'A' and 'meta' or 'B' configurations for $t' = 0.4$ and a finite Lorentzian width $\eta = 0.03$. Bottom: conductance for the 'meta' configuration in the presence of on-site potentials which break the translational invariance. Inset: increase of the weight of the transmission peak through the HOMO as a function of the local potential E_d.

of the system will strongly interact. Such a prediction has been supported by Stepanyuk *et al* [56] who reported results of first-principles calculations of the exchange coupling between magnetic impurities inside quantum corrals.

We present results on the many-body problem of two $S = 1/2$ magnetic impurities located at the foci of elliptical corrals. Each spin interacts via an antiferromagnetic superexchange interaction J with the surface electron spins (figure 5).

We consider the following Hamiltonian:

$$H = H_{\rm el} + J(\vec{S}_1 \cdot \vec{\sigma}_1 + \vec{S}_2 \cdot \vec{\sigma}_2), \tag{6}$$

where

$$\vec{S}_i \cdot \vec{\sigma}_i = S_i^z \cdot \sigma_i^z + \tfrac{1}{2}(S_i^+ \cdot \sigma_i^- + S_i^- \cdot \sigma_i^+), \tag{7}$$

$\sigma_i^+ = c_{i\uparrow}c_{i\downarrow}$, $\sigma_i^z = (n_{i\uparrow} - n_{i\downarrow})/2$, with $n_{i\sigma}$ the number operator and $c_{i\sigma}$ the destruction operator of an electron with spin σ in focus i of the ellipse. In the basis of eigenstates $|\alpha\rangle$ of the isolated ellipse (Mathieu functions), these local operators can be expanded as $c_{i\sigma} = \sum_\alpha \Psi_{\alpha i} c_{\alpha\sigma}$, where $c_{\alpha\sigma}$ and $\Psi_{\alpha i}$ are the destruction operator and amplitude in state $|\alpha\rangle$. $H_{\rm el}$ is the Hamiltonian of the isolated ellipse with infinite walls.

In this basis the spin operators are expressed as

$$\sigma_i^z = \tfrac{1}{2}\sum_{\alpha_1\alpha_2} \Psi^*_{\alpha_1 i}\Psi_{\alpha_2 i}(c^\dagger_{\alpha_1\uparrow}c_{\alpha_2\uparrow} - c^\dagger_{\alpha_1\downarrow}c_{\alpha_2\downarrow}) \qquad \sigma_i^+ = \sum_{\alpha_1\alpha_2} \Psi^*_{\alpha_1 i}\Psi_{\alpha_2 i}c^\dagger_{\alpha_1\uparrow}c_{\alpha_2\downarrow}. \tag{8}$$

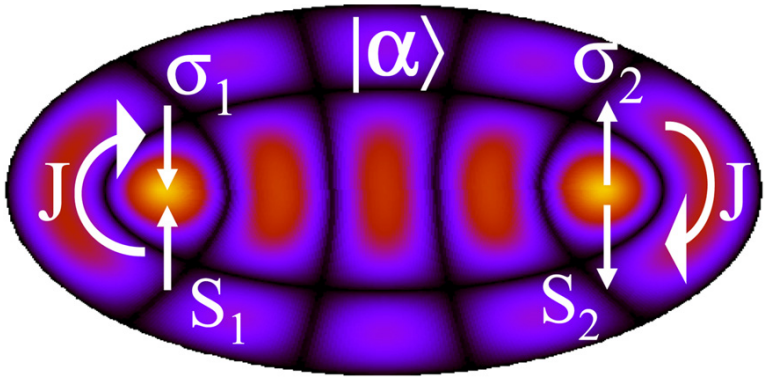

Figure 5. Density of states at the Fermi energy for the non-interacting ellipse with eccentricity $\epsilon = 0.6$. Black lines represent nodal lines of the electronic wavefunction, which has maxima at the foci of the ellipse. Also represented are the eigenstates of the non-perturbed ellipse $|\alpha\rangle$, the impurity spins at the foci of the ellipse, S_1 and S_2, which interact via a antiferromagnetic interaction J with the electronic spins σ_i.

We solve this Hamiltonian numerically using the Lanczos technique for up to ten levels below and above the Fermi level in the ellipse and different fillings corresponding to even (closed shell) or odd (open shell) numbers of particles, N.

We start by analysing two concepts which are widely used in quantum information theory, i.e. the fidelity and the concurrence [57]–[59]. The fidelity measures the quantum transfer from one section of the system to another of a state after a perturbation is applied to the system [59]. It is alternatively defined as the overlap between a time-evolved state and its specular reflection as

$$F_1(t) = |\langle\psi_0|R^\dagger U(t)|\psi_0\rangle| \tag{9}$$

where $U(t) = \mathrm{e}^{-\mathrm{i}Ht}$ is the time evolution operator, H is the perturbed Hamiltonian, $|\psi_0\rangle$ is the eigenstate at the Fermi level and R is the reflection operator along the minor axis of the ellipse in our case.

The concurrence measures the degree of entanglement in the following way:

$$C(t) = \sum_j |\psi(j,t)||R\psi(j,t)|, \tag{10}$$

where $|\psi(j,t)|$ is the time-evolved wavefunction projected on site j.

We calculate these quantities for the non-interacting system (absence of impurities) considering a simplified description of the system, based on a spinless tight-binding model defined on a discretized square lattice within the boundaries of an ellipse, with eccentricity $\epsilon = 0.6$ and hopping element t^* between nearest neighbours. The Hamiltonian in this case is simple and is

$$H_{\mathrm{el}} = -t^* \sum_{\langle i,j\rangle} c_i^\dagger c_j, \tag{11}$$

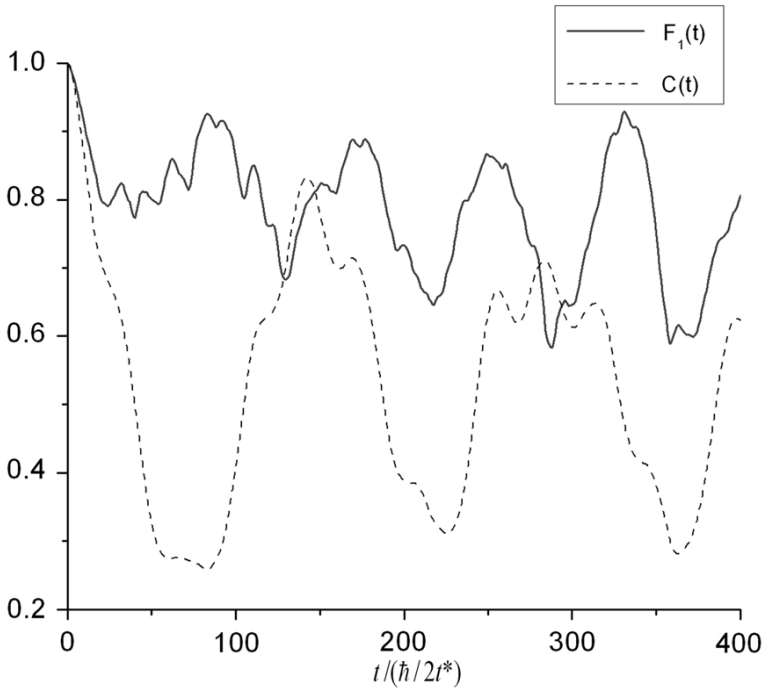

Figure 6. Evolution of the fidelity, F_1, and concurrence, C, for an ellipse without impurities after a potential $e_1 = -1$ is applied at $t = 0$ to focus 1.

where the sites i and j run inside the ellipse which consists of around 1000 sites or atoms. The underlying atomic distribution is irrelevant [31] because we will be analysing low-energy wavefunctions with wavelengths much larger than the real interatomic distance. Our calculations could have also relied on the exact solutions for a non-discretized ellipse (Mathieu functions).

The Fermi energy in our problem coincides with its 23rd eigenstate $|\psi_{23}\rangle$, which is similar to the experimental set-up of [30] (see figure 5). This configuration is not crucial for the main conclusions and other eccentricities and Fermi levels will have a similar behaviour, as long as the wavefunction bears an appreciable weight at the foci of the ellipse.

At time $t = 0$ a negative potential e_1 is applied to the left focus and the dynamical response of the system is observed through these quantities. The results are shown in figure 6.

The initial values of F_1 and C are due to the symmetry of the wavefunction and the time oscillations reflect how accurately the perturbation to the wavefunction is transferred to the other side of the ellipse. This process involves a small number of excited states (states 18 and 23 of the unperturbed Hamiltonian).

We have also studied the time evolution of the ground state when, at time $t = 0$, a constant negative or positive potential V_1 is applied to focus 1: $\exp(-\mathrm{i}Ht)|\psi_0\rangle$, where $H = H_{\mathrm{el}} + V_1(t)$ and $|\psi_0\rangle$ is the ground state of the system with 23 spinless electrons (the spin degree of freedom is irrelevant for this analysis). The square of the amplitude of such

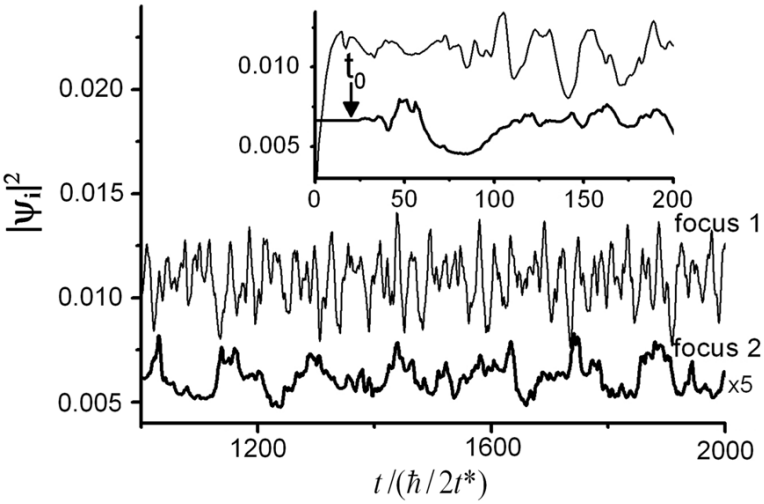

Figure 7. Time evolution of the probability density in both foci for a negative potential, $V_1 = -1$, applied to focus 1 at time $t = 0$. The inset depicts short times. t_0 is the time elapsed until the perturbation reaches the unperturbed focus.

a wavefunction in foci 1 and 2 for $t \geq 0$, for $V_1 = -1$ is shown in figure 7. Here consider $2t^*$ as the energy unit. We notice that a finite time t_0 elapses between the onset of the perturbation in focus 1 and the observation of the response in focus 2, as shown in the inset, which is of the order of $t_0 \sim 20\hbar/2t^* \sim 10^{-14}$ s, where we have used $t^* = 1$ eV. An animated version of this behaviour is found in [60].

Another very important quantity in quantum information is the von Neumann or quantum entropy [57]. Given a quantum system A in a mixed state described by a density operator ρ_A, the quantum entropy is defined as

$$S = -\operatorname{Tr}(\rho_A \log_2 \rho_A). \tag{12}$$

This is a measure of uncertainty in the mixed state. When a system is in a pure state $|\psi\rangle$ and it is divided into two parts, A and B, the entanglement between A and B is defined as the entropy of either part as $E = -\operatorname{Tr}(\rho_A \log_2 \rho_A) = -\operatorname{Tr}(\rho_B \log_2 \rho_B)$, where the density matrices are defined as $\rho^A_{i'i} = \sum_j \psi^*_{ij}\psi_{i'j}$, ψ_{ij} is the projection of the pure state $|\psi\rangle$ onto states i and j corresponding to parts A and B of the system, respectively, and similarly for $\rho^B_{i'i}$. If the density matrices are diagonalized with the eigenvalues ω^A_i, the entropy has a simpler form:

$$S = -\sum_i \omega^A_i \log_2 \omega^A_i = -\sum_i \omega^B_i \log_2 \omega^B_i. \tag{13}$$

To study the entanglement between the spins and the ellipse, we partition our system as shown in the inset of figure 8.

We find that the entropy increases with J and has a slightly different behaviour for even and odd particles in the ellipse (figure 8). For even filling in the ellipse and small interaction, the entropy is negligible because the spins are locked into a singlet state and the ground state consists of a direct product between this singlet and the ground state

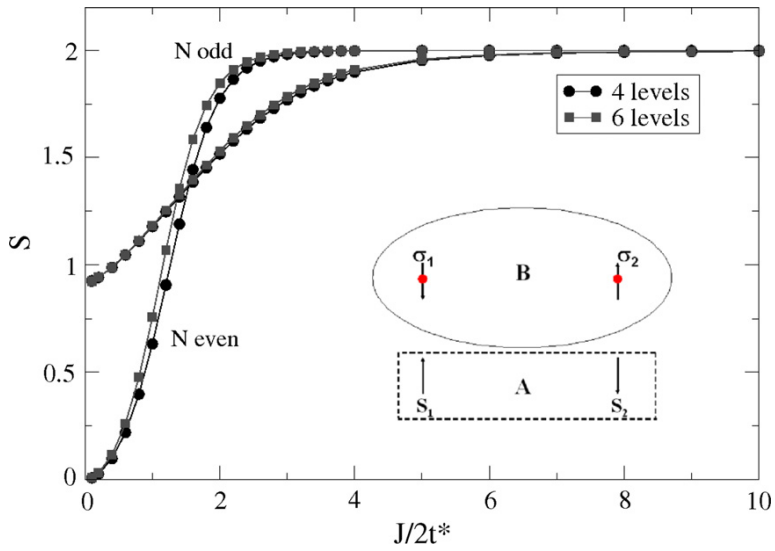

Figure 8. Entanglement entropy as a function of the interaction for the partition shown in the inset. A contains the localized spins and B the extended electrons.

of the non-interacting ellipse. When J increases, more states get involved, the localized spins are no longer in a singlet and the entropy or entanglement increases. In the largest entangled case we have in A a sum of all four spin states ($|\uparrow\uparrow\rangle$, $|\uparrow\downarrow\rangle$, $|\downarrow\uparrow\rangle$, $|\downarrow\downarrow\rangle$), which appear with equal probability. For odd fillings and small J, the spins are in a mixture of mainly two triplet states because we are considering the $S^z_{\rm T} = 1/2$ subspace. For large J, the results match the even case and have maximum entropy ($S = \log_2 4 = 2$).

Now we analyse a different partition of the system and consider the entanglement between both localized impurities. To analyse this entanglement, we have to resort to the formulation performed by Wootters for the entanglement between two qubits in a mixed state (since the localized impurities are no longer in a pure state once they interact with the ellipse) [58]: $E(C) = h((1+\sqrt{1-C^2})/2)$, where $h(x) = -x\log_2 x - (1-x)\log_2(1-x)$ and C is the concurrence $C(\rho) = \max\{0, \lambda_1 - \lambda_2 - \lambda_3 - \lambda_4\}$. λ_i are the eigenvalues of the Hermitian matrix $R = \sqrt{\sqrt{\rho}\rho^*\sqrt{\rho}}$, where $\rho^* = (\sigma_y \otimes \sigma_y)\rho^*(\sigma_y \otimes \sigma_y)$, σ_y is the Pauli matrix and ρ is the reduced density matrix of the magnetic impurities.

In figure 9 we show the entanglement between the impurities as a function of the interaction J. We see that, as expected, the quantum entanglement E is maximal for small J values. For even electrons the localized spins are locked in a singlet state with the highest entanglement between them (and lowest with the corral electrons). For odd fillings the entanglement is smaller due to the fact that we have fixed the subspace $S^z_{\rm T} = -1/2$ in the whole system and here the triplet ground state has contributions of the 0 and -1 projections of the localized triplets. For all fillings, the entanglement goes to zero for large interactions (i.e. large mixing with the electronic levels).

We note that the discontinuity observed in the derivative of E for $J \simeq 1.5$ and 2 is due to the definition of the concurrence given above [58] and does not signal any level crossing. This discontinuity can be removed by using the 'quantum discord' magnitude instead [61, 62].

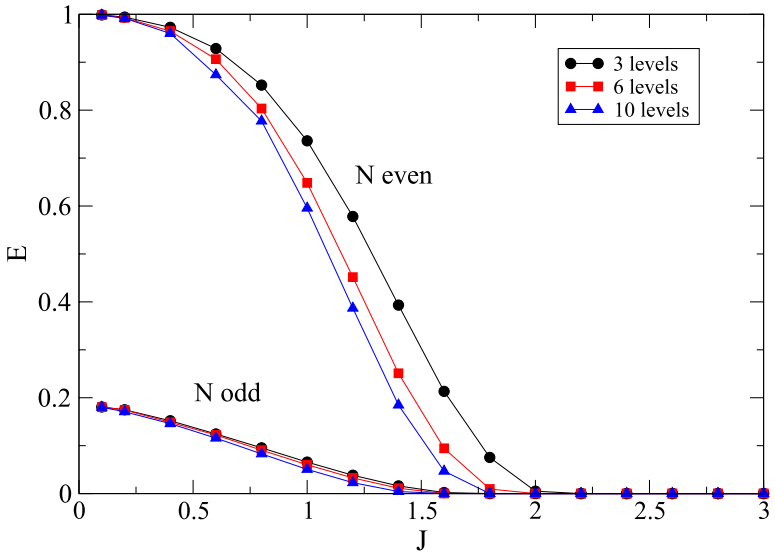

Figure 9. Entanglement between the localized impurities as a function of the interaction for even and odd fillings and different numbers of levels considered.

4. Conclusions

We have shown how some basic and interesting quantum physical behaviour could be observed in modern nanoscopic systems. Quantum coherence can be crucial in transport properties through conjugated molecules such as benzene to the point of producing important switching effects between high and low conducting states. For some molecules, a switch between non-conducting and conducting states occurs when a perturbation which breaks the molecular symmetry is applied to the system, thus disrupting destructive interference effects.

Strong correlations between electrons also have fundamental effects in the low-energy basic excitations of low-dimensional systems: they lead to the separation of spin and charge degrees of freedom. This phenomenon could also be directly observed by transport measurements through strongly interacting nanoscopic rings pierced by a magnetic field in an Aharonov–Bohm configuration: the conductance will show clear dips at fractional values of the magnetic flux, the position of which corresponds, mainly, to the ratio of the charge and spin velocities and to the position of the leads.

Finally, quantum corrals are an ideal playground to study and measure quantum entanglement. The focalizing properties of elliptic corrals enhance the correlations of magnetic impurities localized in its foci allowing for robust and strongly entangled magnetic states at low temperatures which could be of interest for possible applications in quantum computing.

Acknowledgments

This work was done in the framework of projects PIP 5254 of CONICET, PICT 2006/483 of the ANPCyT and the ARG/RPO-041/2006 Indo-Argentine collaboration. SR thanks DST for support through a JC Bose fellowship.

References

[1] Goldhaber-Gordon D, Shtrikman H, Mahalu D, Abusch-Magder D, Meirav U and Kastner M A, 1998 *Nature* **391** 156
[2] Cronenwet S M, Oosterkamp T H and Kouwenhoven L P, 1998 *Science* **281** 540
[3] Goldhaber-Gordon D, Göres J, Kastner M A, Shtrikman H, Mahalu D and Meirav U, 1998 *Phys. Rev. Lett.* **81** 5225
[4] van der Wiel W G, de Franceschi S, Fujisawa T, Elzerman J, Tarucha S and Kowenhoven L P, 2000 *Science* **289** 2105
[5] Grobis M, Rau I G, Potok R M, Shtrikman H and Goldhaber-Gordon D, 2008 *Phys. Rev. Lett.* **100** 246601
[6] Rincón J, Aligia A A and Hallberg K, 2009 *Phys. Rev.* B **79** 121301(R)
Rincón J, Aligia A A and Hallberg K, 2009 *Phys. Rev.* B **80** 079902(E)
Rincón J, Aligia A A and Hallberg K, 2010 *Phys. Rev.* B **81** 039901(E)
[7] Roura-Bas P, 2010 *Phys. Rev.* B **81** 155327
[8] Nishikawa Y, Crow D J G and Hewson A C, 2010 *Phys. Rev.* B **82** 115123
[9] Kouwenhoven L P, Hekking F, van Wees B, Harmans B, Timmering C and Foxon C, 1990 *Phys. Rev. Lett.* **65** 361
[10] Oreg Y and Goldhaber-Gordon D, 2003 *Phys. Rev. Lett.* **90** 136602
[11] Žitko R and Bonča J, 2006 *Phys. Rev.* B **74** 224411
[12] Aligia A A, Hallberg K, Normand B and Kampf A P, 2004 *Phys. Rev. Lett.* **93** 076801
[13] Martins G, Büsser C, Al-Hassanieh K, Moreo A and Dagotto E, 2005 *Phys. Rev. Lett.* **94** 026804
[14] Dias da Silva L, Sandler N, Ingersent K and Ulloa S, 2006 *Phys. Rev. Lett.* **97** 096603
Dias da Silva L, Sandler N, Ingersent K and Ulloa S, 2007 *Phys. Rev. Lett.* **99** 209702
Vaugier L, Aligia A and Lobos A M, 2007 *Phys. Rev. Lett.* **99** 209701
[15] Vaugier L, Aligia A A and Lobos A M, 2007 *Phys. Rev.* B **76** 165112
[16] Jagla E A, Hallberg K and Balseiro C A, 1993 *Phys. Rev.* B **47** 5849
[17] Aviram A and Ratner M A, 1974 *Chem. Phys. Lett.* **29** 277
[18] Reed M A *et al*, 1997 *Science* **278** 252
[19] Cuniberti G, Fagas G and Richter K (ed), 2005 *Introducing Molecular Electronics* (Berlin: Springer)
[20] Rincón J, Hallberg K, Aligia A A and Ramasesha S, 2009 *Phys. Rev. Lett.* **103** 266807
[21] Nitzan A and Ratner M A, 2003 *Science* **300** 1384
[22] Tao N, 2006 *Nat. Nanotechnol.* **1** 173
[23] Cardamone D *et al*, 2006 *Nano Lett.* **6** 2422
[24] Ke S H *et al*, 2008 *Nano Lett.* **8** 3257
[25] Yeganeh S *et al*, 2009 *Nano Lett.* **9** 1770
[26] Park J *et al*, 2002 *Nature* **417** 722
[27] Venkataraman B *et al*, 2006 *Nature* **442** 904
[28] Danilov A V *et al*, 2008 *Nano Lett.* **8** 1
[29] Dadosh T *et al*, 2005 *Nature* **436** 677
[30] Manoharan H C, Lutz C P and Eigler D, 2000 *Nature* **403** 512
[31] Fiete G and Heller E, 2003 *Rev. Mod. Phys.* **75** 933
[32] Aligia A A and Lobos A M, 2005 *J. Phys.: Condens. Matter* **17** S1095
[33] Zutic I, Fabian J and Das Sarma S, 2004 *Rev. Mod. Phys.* **76** 32
[34] Awschalom D, Loss D and Samarth N (ed), 2002 *Semiconductor Spintronics and Quantum Computation* (Berlin: Springer)
[35] Kollath C, Schollwoeck U and Zwerger W, 2005 *Phys. Rev. Lett.* **95** 176401
[36] White S, 1992 *Phys. Rev. Lett.* **69** 2863
Hallberg K, 2006 *Adv. Phys.* **55** 477
Schollwoeck U, 2005 *Rev. Mod. Phys.* **77** 259
Peschel I, Wang X, Kaulke M and Hallberg K (ed), 1998 *Lecture Notes in Physics* (Berlin: Springer)
[37] Jagla E A and Balseiro C A, 1993 *Phys. Rev. Lett.* **70** 639
[38] Friederich S and Meden V, 2008 *Phys. Rev.* B **77** 195122
[39] Hallberg K, Aligia A A, Kampf A and Normand B, 2004 *Phys. Rev. Lett.* **93** 067203
[40] Rincón J, Aligia A A and Hallberg K, 2009 *Phys. Rev.* B **79** 035112
[41] Rincón J, Aligia A A and Hallberg K, 2009 *Physica* B **404** 2270
[42] Rincón J, Hallberg K and Aligia A A, 2009 *Physica* B **404** 3147
[43] Rincón J, Hallberg K and Aligia A A, 2008 *Phys. Rev.* B **78** 125115

J. Stat. Mech. (2010) P11031

[44] Davidson E R, 1975 *J. Comput. Phys.* **17** 87
Davidson E R, 1989 *Comput. Phys. Commun.* **53** 49
[45] Ogata M and Shiba H, 1990 *Phys. Rev.* B **41** 2326
[46] Caspers W and Ilske P, 1989 *Physica* A **157** 1033
Schadschneider A, 1995 *Phys. Rev.* B **51** 10386
[47] Pariser R and Parr R, 1953 *J. Chem. Phys.* **21** 466
Pople J A, 1953 *Trans. Faraday Soc.* **49** 1375
[48] Ohno K, 1964 *Theor. Chim. Acta* **2** 219
[49] Soos Z G and Ramasesha S, 1984 *Phys. Rev.* B **29** 5410
[50] Hallberg K, Correa A and Balseiro C, 2002 *Phys. Rev. Lett.* **88** 066802
[51] Correa A, Hallberg K and Balseiro C, 2002 *Europhys. Lett.* **58** 6
[52] Chiappe G and Aligia A A, 2002 *Phys. Rev.* B **66** 075421
Chiappe G and Aligia A A, 2004 *Phys. Rev.* B **70** 129903(E)
[53] Nizama M, Hallberg K and d'Albuquerque e Castro J, 2007 *Phys. Rev.* B **75** 235445
Nizama M, Hallberg K and d'Albuquerque e Castro J, 2008 *Microelectron. J.* **39** 1289
[54] Hallberg K and Nizama M, 2008 *Prog. Theor. Phys.* **176** 408
[55] Nizama M, Frustaglia D and Hallberg K, 2009 *Physica* B **404** 2819
[56] Stepanyuk V S, Niebergall L, Hergert W and Bruno P, 2005 *Phys. Rev. Lett.* **94** 187201
[57] Nielsen M and Chuang I, 2000 *Quantum Computation and Quantum Information* (Cambridge: Cambridge University Press)
[58] Wootters W K, 1998 *Phys. Rev. Lett.* **80** 2245
[59] Qian X F, Li Y, Song Z and Sun C P, 2005 *Phys. Rev.* A **72** 062329
[60] http://fisica.cab.cnea.gov.ar/solidos/personales/hallberg/ellipse_time_evolution_v1=1.mpeg
[61] Ollivier H and Zurek W H, 2001 *Phys. Rev. Lett.* **88** 017901
[62] Luo S, 2008 *Phys. Rev.* A **77** 042303

J. Stat. Mech. (2010) P11031